Real-Time Simulation of Three-Phase Transmission Lines Modeled in the Dynamic Harmonic Domain

Jose de Jesus Chavez[1], Manuel Madrigal[1], Venkata Dinavahi[2]
[1]Instituto Tecnologico de Morelia, Mexico
[2]University of Alberta, Canada
jchavez@gdl.cinvestav.mx, manuelmadrigal@ieee.org, dinavahi@ece.ualberta.ca.

Abstract— **This paper presents a real-time simulation of transmission lines including harmonics in dynamic state. The Dynamic Harmonic Domain (DHD) transmission line model used in this work is based in a frequency dependent line model in the phase domain. The advantages of using the DHD methodology are: its capability to accurately follow the harmonic content of a transient without the aid of a post-processing tool and its ability to serve as a visually active indicator of steady-state and transient condition in a signal. The DHD transmission line model is implemented in a real time simulator in order to reduce the simulation time.**

The real-time simulation of an illustrative example, involving fast transients in transmission lines has been achieved with a maximum computation time of 0.5s on a step-size of 10 μs. The case study results were validated against those obtained through a time domain off-line simulation.

keywords— **Electromagnetic transients, Harmonic analysis, Real-Time simulation, Transmission line.**

I. INTRODUCTION

TRANSMISSION line models constitute major components in the analysis of electromagnetic transients in power systems. Such models are usually formulated either in the frequency domain or in the time domain, some important contributions in this area are [1] - [6]. Using any of those models, one can obtain voltages and currents as function of time. The inclusion of elements that produce and introduce distortions to the power signals makes the analysis of the harmonic content of such waves attractive, especially when nonlinear loads and/or electronic devices are connected to the system. In addition, the consideration of harmonics in a transmission line/nonlinear load system is desirable when assessing resonance conditions [7], [8].

This research work proposes the real time application of the model developed in [9] where the DHD transmission line model was proposed. It consists of a combination of the traveling waves approach and the modified dynamic harmonic domain technique [10], [11]. The latter consists on representing a time-varying quantity by the Fourier transform (FT) whose coefficients are allowed to vary

J. J. Chavez and M. Madrigal are with the Instituto Tecnologico de Morelia, Mexico.

V. Dinavahi is with the Dept. of Electrical & Computer Engineering at the University of Alberta, Canada.

slowly within a time span. Accounting for enough harmonics, the DHD permits to follow in a step-by-step fashion the voltage/current harmonics behavior with respect to time in a precise manner.

By its nature, the DHD analysis involve large dynamic system equations which are solved using real-time simulation in this paper. The simulator used is an integral component of the Real-Time eXperimental Laboratory (RTX-Lab) in the Power Engineering Group at the University of Alberta.

Another advantage of real-time simulators is their capability to communicate with physical hardware such as digital controllers and protective relays. This feature, called hardware-in-the-loop (HIL) simulation, allows such equipment to be designed, tested, and validated under realistic system conditions before being placed in the field [12], [13]. Applications that make this simulation worthy to conduct include the study of harmonics in transient state for control, protection, power quality purposes, and also the potential study of resonance.

The paper is organized as follows: In Section II the dynamic harmonic domain (DHD) basic theory is briefly described. Section III describes the Time Domain (TD) and DHD modeling of frequency dependent transmission lines. Real-time implementation features are presented in Section IV. Section V presents the numerical results corresponding to the case of study.

II. DYNAMIC HARMONIC DOMAIN THEORY

In this section, the conversion of an ODE from TD to DHD is described [9]- [11]. This will set the basis for the line modeling which involves ODEs.

Without loss of generality, consider the linear time periodic (LTP) system for the scalar case

$$\dot{x}(t) = a(t)x(t) + b(t)u(t), \tag{1a}$$
$$y(t) = c(t)x(t) + d(t)u(t). \tag{1b}$$

Consider also that any variable (or coefficient) in (1) can be expressed by its Fourier series with corresponding coefficients assumed to be time-varying. For example, $x(t)$ can be defined as

$$x(t) = x_{-h}(t)e^{-jh\omega_o t} + \cdots + x_{-1}(t)e^{-j\omega_o t} + x_o(t)$$
$$+ x_1(t)e^{j\omega_o t} + \cdots + x_h(t)e^{jh\omega_o t}. \quad (2)$$

By expressing all the variables from (1) by the Fourier series, as in (2), and by dropping all the exponential factors, the state representation of (1) in the DHD becomes

$$\dot{\mathbf{x}} = (\mathbf{A} - \mathbf{S})\mathbf{x} + \mathbf{B}\mathbf{u}, \quad (3a)$$
$$\mathbf{y} = \mathbf{C}\mathbf{x} + \mathbf{D}\mathbf{u}, \quad (3b)$$

The variables in (3), have been arranged as harmonic vectors with complex time-varying elements, for instance $\mathbf{x}$ is defined as:

$$\mathbf{x} = [x_{-h}(t), \cdots, x_{-1}(t), x_o(t), x_1(t), \cdots, x_h(t)]^T, \quad (4)$$

where T denotes the transpose. The diagonal matrix $\mathbf{S}$ is called the operational matrix of differentiation defined in [1] by:

$$\mathbf{S} = diag\{-jh\omega_o, \cdots, -jh\omega_o, 0, j\omega_o, \cdots, jh\omega_o\}, \quad (5)$$

where h is the maximus harmonic taken into account.

It is worthy to mention that the derivatives in TD are represented in the DHD as:

$$(TD) \quad \dot{x} \Leftrightarrow \dot{\mathbf{x}} + \mathbf{S}\mathbf{x} \quad (DHD). \quad (6)$$

In addition, matrix $\mathbf{A}$ (as well as $\mathbf{B}$, $\mathbf{C}$, and $\mathbf{D}$) the harmonic coefficients of $a(t)$ in a Toeplitz-type structure as follows:

$$\mathbf{A} = \begin{bmatrix} a_o & \cdots & a_h & & \\ \vdots & \ddots & & a_h & \\ & & & & \\ a_{-h} & & \ddots & \vdots \\ & a_{-h} & \cdots & a_o \end{bmatrix}. \quad (7)$$

Note that since (1) has been considered as LTP, the coefficient matrices in the DHD system given by (3) now become constant matrices, as in (7), thus (3) represents a linear time invariant (LTI) system [11].

The system of coupled ODEs in (3) has dimension of $2h + 1$ and it becomes decoupled (diagonal) when dealing with an LTI system (i.e., a, b, c, and d being constant). Furthermore, the dimensions can be reduced to $h + 1$ when considering half-wave symmetry; that is, when only odd harmonics are considered due to sinusoidal sources. Although in this work is presented linear loads the DHD can handle nonlinear loads in a straightforward manner, as was presented in a previous work [9].

III. TRANSMISSION LINE IN THE DHD

Since the underlying idea of this work is to analyze transients accurately, the DHD transmission line model used here is based on a frequency dependent distributed parameters model.
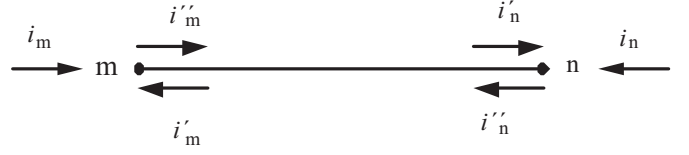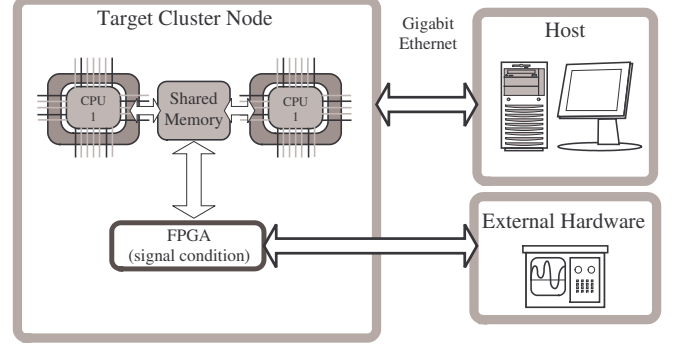

Fig. 1.   Transmission line reference directions.

Fig. 2.   Configuration of the real-time simulator.

A. Traveling Wave Method in the TD

Considering the reference directions for a three phase transmission line as depicted in Fig. 1, the Frequency Domain (FD) relations between incident currents (i') and reflected currents (i'') for both ends of the line (and for a given mode) are:

$$i'_m = H_{mode}i''_n, \quad (8a)$$
$$i'_n = H_{mode}i''_m, \quad (8b)$$

where H_{mode} represents the modal propagation function. Approximating H_{mode} by rational functions [4], we can express (8) as:

$$i'_m = [\mathbf{c}_1(s\mathbf{I} - \mathbf{a}_1)^{-1}\mathbf{b}_1]i''_n, \quad (9a)$$
$$i'_n = [\mathbf{c}_1(s\mathbf{I} - \mathbf{a}_1)^{-1}\mathbf{b}_1]i''_m. \quad (9b)$$

In (9), the set of poles (k poles), obtained from the rational fitting, are contained in the diagonal matrix $\mathbf{a}_1$ of dimensions $k \times k$; the column vector $\mathbf{b}_1 (k \times 1)$ has all entries equal to 1, and the residues of the realization are contained in the row vector $\mathbf{c}_1 (1 \times k)$. Additionally, s represents the complex frequency given by $s = \alpha + j\omega$. From (9) we define:

$$x_1 = (s\mathbf{I} - \mathbf{a}_1)^{-1}\mathbf{b}_1 i''_n, \quad (10a)$$
$$x_2 = (s\mathbf{I} - \mathbf{a}_1)^{-1}\mathbf{b}_1 i''_m. \quad (10b)$$

Now, the TD image of (10) becomes

$$\dot{x}_1 = \mathbf{a}_1 x_1 + \mathbf{b}_1 i''_n, \quad (11a)$$
$$\dot{x}_2 = \mathbf{a}_1 x_2 + \mathbf{b}_1 i''_m. \quad (11b)$$

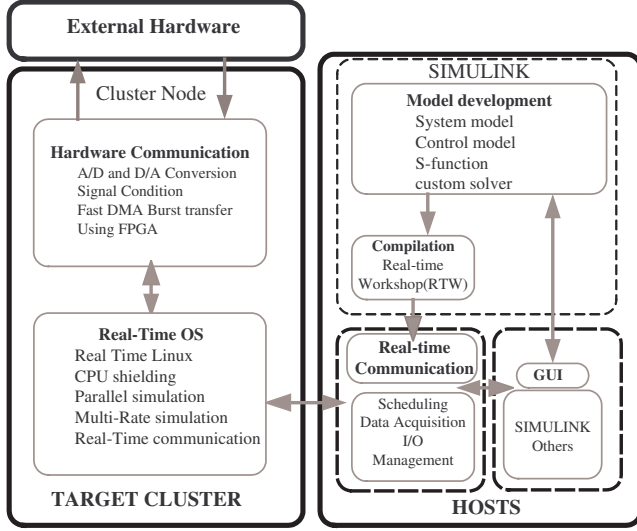Thus, the state-space realization for the two line nodes (m, n) is:

Fig. 3. Functional block diagram of software used in the real-time simulator.
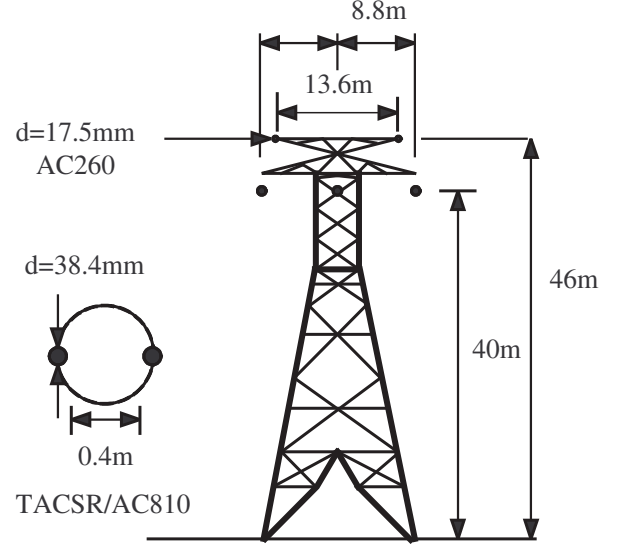

Fig. 4. Transmission line geometrical configuration.

$$\begin{bmatrix} \dot{x}_1 \\ \dot{x}_2 \end{bmatrix} = \begin{bmatrix} \mathbf{a}_1 & \\ & \mathbf{a}_1 \end{bmatrix} \begin{bmatrix} x_1 \\ x_2 \end{bmatrix} + \begin{bmatrix} \mathbf{b}_1 & \\ & \mathbf{b}_1 \end{bmatrix} \begin{bmatrix} i_n'' \\ i_m'' \end{bmatrix}, \tag{12a}$$

$$\begin{bmatrix} i_n' \\ i_m' \end{bmatrix} = \begin{bmatrix} \mathbf{c}_1 & \\ & \mathbf{c}_1 \end{bmatrix} \begin{bmatrix} \mathbf{x}_1 \\ \mathbf{x}_2 \end{bmatrix}. \tag{12b}$$

It is mentioned here that the reflected currents i_n'' and i_m'' are calculated at time $t - \tau$, with τ being the travel time. Additionally, the terminal relations in phase domain between currents and voltages are described by:

$$\mathbf{Y}_c v_m - i_m = 2i_m', \tag{13a}$$

$$\mathbf{Y}_c v_n - i_n = 2i_n', \tag{13b}$$

where $\mathbf{Y}_c$ corresponds to the characteristic admittance of the line, being also approximated by rational functions. Following a similar procedure, the state-space representation of (13a) is given as:

$$\dot{x}_3 = \mathbf{a}_2 x_3 + \mathbf{b}_2 \mathbf{v}_m, \tag{14a}$$

$$i_m = \mathbf{c}_2 x_3 + \mathbf{d}_2 \mathbf{v}_m - 2i_m', \tag{14b}$$

and (13b) is given as:

$$\dot{x}_4 = \mathbf{a}_2 x_4 + \mathbf{b}_2 \mathbf{v}_n, \tag{15a}$$

$$i_n = \mathbf{c}_2 x_4 + \mathbf{d}_2 \mathbf{v}_n - 2i_n', \tag{15b}$$

B. Traveling Wave Method in the DHD

Since (12) corresponds to a set of linear ODEs, its DHD counterpart is easily found as:

$$\begin{bmatrix} \dot{\mathbf{x}}_1 \\ \dot{\mathbf{x}}_2 \end{bmatrix} = \begin{bmatrix} \mathbf{A}_1 - \mathbf{S}' & \\ & \mathbf{A}_1 - \mathbf{S}' \end{bmatrix} \begin{bmatrix} \mathbf{x}_1 \\ \mathbf{x}_2 \end{bmatrix} + \begin{bmatrix} \mathbf{B}_1\Gamma & \\ & \mathbf{B}_1\Gamma \end{bmatrix} \begin{bmatrix} \mathbf{i}_n'' \\ \mathbf{i}_m'' \end{bmatrix}, \tag{16a}$$

$$\begin{bmatrix} \mathbf{i}_m' \\ \mathbf{i}_n' \end{bmatrix} = \begin{bmatrix} \mathbf{C}_1 & \\ & \mathbf{C}_1 \end{bmatrix} \begin{bmatrix} \mathbf{x}_1 \\ \mathbf{x}_2 \end{bmatrix}. \tag{16b}$$

The size and the arrangement of the state-realization in the DHD differ from the TD formulation. Based on (4), (5), and (16), in the DHD we have the following definitions with corresponding dimensions shown in round parentheses:

$$\mathbf{A}_1 = diag\{\mathbf{a}_1\mathbf{I}_d, \mathbf{a}_2\mathbf{I}_d, \dots \mathbf{a}_k\mathbf{I}_d\}, (kh \times kh), \tag{17a}$$

$$\mathbf{S}' = diag\{\mathbf{S}, \mathbf{S}, \dots \mathbf{S}\}, (kh \times kh), \tag{17b}$$

$$\mathbf{B}_1 = [\mathbf{I}_d, \mathbf{I}_d, \dots, \mathbf{I}_d]^T, (kh \times h), \tag{17c}$$

$$\mathbf{C}_1 = [c_1\mathbf{I}_d, c_2\mathbf{I}_d, \dots, c_k\mathbf{I}_d], (h \times kh). \tag{17d}$$

In addition, the time delay for all harmonics is taking into account by:

$$\Gamma = diag\{e^{jh\omega_o\tau}, \dots, e^{j\omega_o\tau}, 1, e^{-j\omega_o\tau}, \dots, e^{-jh\omega_o\tau}\}. \tag{18}$$

Following a similar procedure, the DHD state-space representation of (14) and (15) are:

$$\dot{\mathbf{x}}_3 = (\mathbf{A}_2 - \mathbf{S}')\mathbf{x}_3 + \mathbf{B}_2\mathbf{v}_m, \tag{19a}$$

$$\mathbf{i}_m = \mathbf{C}_2\mathbf{x}_3 + \mathbf{D}_2\mathbf{v}_m - 2i_m', \tag{19b}$$

and

$$\dot{\mathbf{x}}_4 = (\mathbf{A}_2 - \mathbf{S}')\mathbf{x}_4 + \mathbf{B}_2\mathbf{v}_n, \tag{20a}$$

$$\mathbf{i}_n = \mathbf{C}_2\mathbf{x}_4 + \mathbf{D}_2\mathbf{v}_n - 2i_n', \tag{20b}$$

respectively; where $\mathbf{A}_2$, $\mathbf{B}_2$, $\mathbf{C}_2$ are defined in accordance with (17a)-(17d) and $\mathbf{D}_1 = d_1\mathbf{I}_h$. In addition to the propagation equations (12) and the terminal relations (19) and (20), we have to consider the terminations of the line. Finally, after calculating $\mathbf{i}_m$ and $\mathbf{i}_n$ from (19b) and (20b) respectively, the reflected currents are updated with

$$\mathbf{i}''_n = \mathbf{i}'_n + \mathbf{i}_n, \tag{21a}$$

$$\mathbf{i}''_m = \mathbf{i}'_m + \mathbf{i}_m. \tag{21b}$$

The solution for each load node can be calculated by using the nodal elimination (20). Finally, the reflected currents are updated. In the case of a network with several transmission lines, the procedure described above could be used. The incident currents are calculated for each line using an expression similar to (16).

IV. Real-Time Implementation

To reduce the amount of time and computational resources needed the transmission line model was coded entirely in C language and embedded as a dynamically linked program (S-function) in SIMULINK to be simulated in a real time environmental. In this section the details of the real-time simulator from Opal® used in the RTX-Lab [14] are presented.

A. Hardware

Fig. 2 shows the hardware architecture of the real-time simulator. The simulator has been built on eight high-speed computer cluster nodes (known as the target) The target cluster is considered as the heart of the real-time simulator. Each node is composed by two 3.0GHz dual Intel Xeon processors capable to run interactively or independently. The simulator also consists on a group of computers used for the model development, compilation, and loading the compiled programs to the cluster nodes [15], [16].

Additionally, real world hardware such as digital controllers, protective relays, and power electronic devices can be interfaced with the target cluster through the FPGA-based multichannel I/O modules. The physical interaction between all the real-time components have been addressed by one o several corresponding communication technologies: shared memory, infinity band link, signal wire link, and gigabit Ethernet link.

B. Software

Fig. 3 shows the software architecture of the real-time simulator [15], [16]. It is divided in target cluster and host. The target cluster runs on RedHawk Linux. At the target cluster real-time execution and data acquisition, recording and sending from/to the host is performed. The host could be running either in Windows or Linux OS. The real-time simulator host uses Windows XP and Matlab/SIMULINK environment. Matlab/SIMULINK is employed for the development of power and control system models. Most
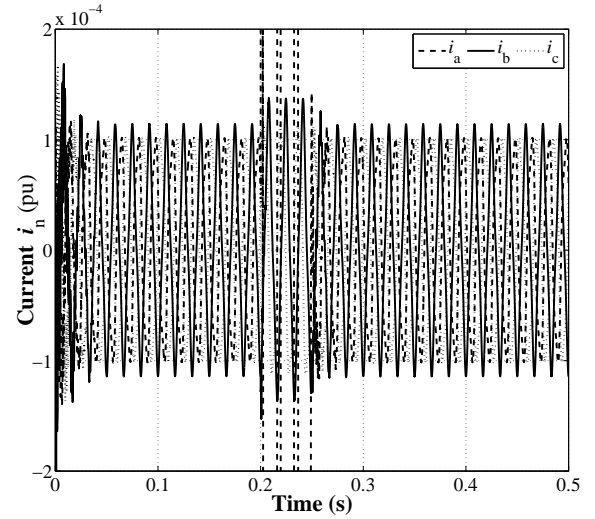
(a)
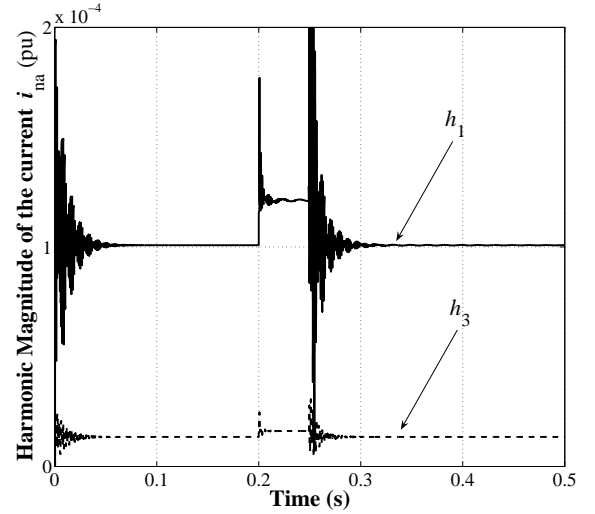
(b)

Fig. 5. (a) Current at sending node i_n (pu), and (b) Harmonic magnitude of the current i_{ma}.

physical systems and their control can be modeled with the built-in Matlab/SIMULINK tool-boxes; however, user-defined models and solver algorithms written in Matlab or other high level languages, such as C/C++ or Fortran, can also be included through the Matlab/SIMULINK S-function interface. Large systems can be divided into several subsystems and distributed over parallel operating cluster nodes. Additionally, Matlab/SIMULINK environment provides the user with interfacing tools to monitoring and controlling the inputs/outputs of real-time simulations and control.

V. Case Study

The 100km untransposed transmission line under analysis (see Fig.4 for geometrical details) is connected to a source $v_o = \sin(\omega_o t) + \frac{1}{8}\sin(3\omega_o t)\,pu$ at one of its ends

and at the other an identical linear load admittance $Y_L = 0.0001$ pu is connected.

The simulation starts assuming initial conditions equal to zero. Then at $t = 0$s the source is connected to the transmission line. After 0.2s a single-phase fault is simulated through the connection of an admittance ($Y_L = 10e^4$ pu) to ground at phase b. Then after the third cycle (0.249 s) the fault is cleared and the same admittance before the fault is connected until a new steady state is reached. The simulation ends at 0.5s.

Fig. 6 shows the instantaneous receiving end voltage v_n obtained by the DHD-Real-time simulation. One can observe the distortion produced by the two transients, a zoom is done to show the second transient at the moment when the fault is cleared.

Fig. 5a depicts the instantaneous current at the end of the transmission line. Accordingly, Fig. 5b shows the phase b harmonic behavior during the whole observation time. One can observe that the harmonics oscillate with the power frequency. The attenuation of this oscillation indicates the end of the transient state and depends of the transmission line length and the network configuration.

The results obtained by the DHD-Real-time simulation were compared with those obtained by the direct simulation of the ODEs system in the time-domain. In Fig. 7 a) the current i_{ma} is shown and a comparison between the TD-offline and the DHD-Real-time simulation (labeled as dashed and continuous line respectively) is done. The difference between both methodologies is almost unnoticeable.

Some remarks regarding the obtained results (see Fig.5b and Fig.7b) :

1) During steady state all harmonics behave as constants, as expected.
2) Harmonics react instantaneously to system disturbances. Their dynamics are followed in a natural way by the DHD whilst post-processing techniques (for instance, WFFT) would have a slow harmonic tracking response.
3) The proportionality of harmonic magnitudes for a given signal (voltage or current) changes from steady-state to the transient state.
4) Harmonic oscillations during a transient behave according to the line resonant frequency, traveling time, and excitation related frequencies.
5) After removing a fault, steady state is reached faster by lower harmonics than by higher harmonics.
6) Simply examining the time-domain results it is difficult to discern the steady-state condition. The DHD provides a visually active indicator of the transient and steady-state conditions in a signal.

VI. Conclusions

This paper has presented the real-time simulation of an untransposed transmission line for analyzing harmonics behavior under transient conditions. The transmission line was modeled in the dynamic harmonic domain (DHD)
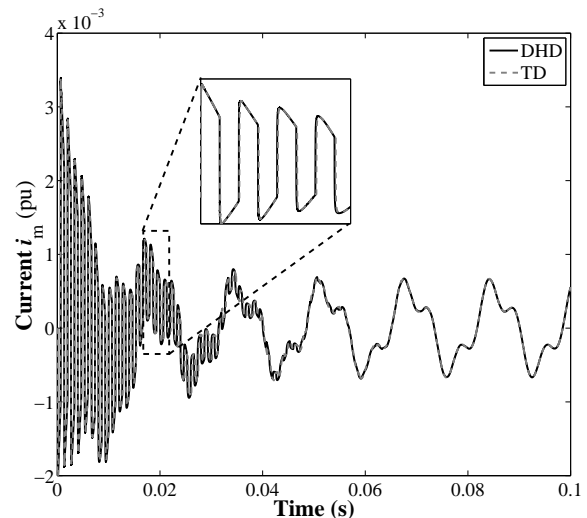
(a)
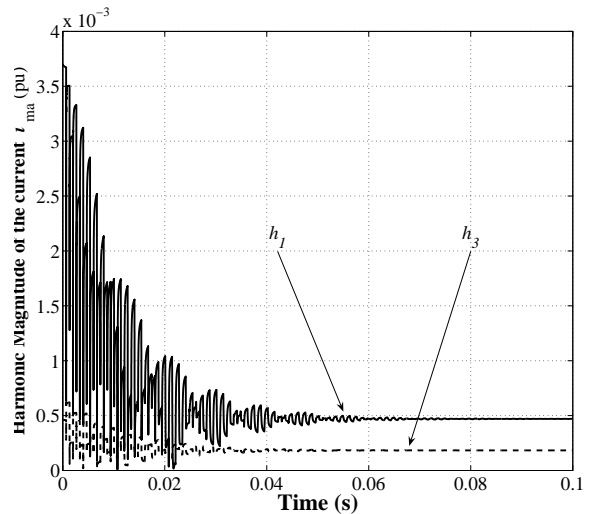
(b)

Fig. 7. (a) Current i_n (pu), and (b) Harmonic magnitude of the voltage v_{na}.

which permits to follow step-by-step the harmonics evolution with respect to time. Additionally, it has been corroborated that the time-varying harmonic coefficients are capable of representing the non-harmonic line frequencies involved in the transient. The DHD can handle nonlinear loads in a straightforward manner (as was presented in a previous work [9])whilst in frequency domain techniques the inclusion of such loads is still difficult. The accuracy of the model was verified doing a comparison with the TD solution. To overcome the computational problem due to the ODEs DHD size, a real-time simulation was performed. The applications of the algorithm include the study of harmonics in transient state for control, protection, power quality purposes, and also in the study of ferroresonance.

References

[1] A. Semlyen and A. Dabuleanu, "Fast and accurate switching transient calculations on transmission lines with ground return
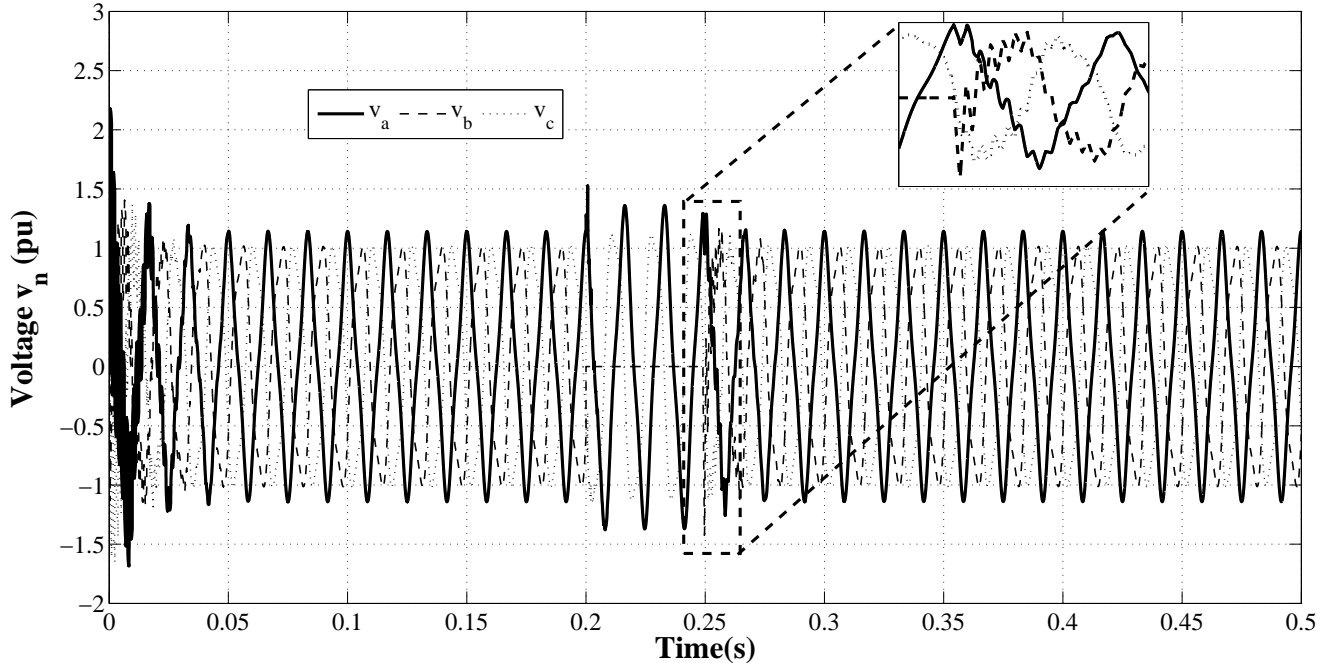
Fig. 6.   Receiving end voltage v_n (pu).

using recursive convolutions", *IEEE Trans. Power Apparatus and Systems,* vol. PAS-94, no. 2, March/April 1975, pp. 561-571.
[2] J. R. Marti, "Accurate modeling of frequency-dependent transmission lines in electromagnetic transient simulations", *IEEE Trans. Power Apparatus and Systems,* vol. PAS-101, no. 1, January 1982, pp. 147-157.
[3] H. V. Nguyen, H. W. Dommel, and J. R. Marti, "Direct phase-domain modeling of frequency-dependent overhead transmission lines", *IEEE Trans. Power Delivery,* vol. 12, no. 3, July 1997, pp. 1335-1342.
[4] F. Castellanos and J. R. Marti, "Full frequency-dependent phase-domain transmission line model", *IEEE Trans. Power Systems,* vol. 12, no. 3, August 1997, pp. 1331-1339.
[5] B. Gustavsen and A. Semlyen, "Combined phase domain and modal domain calculation of transmission line transients based on vector fitting", *IEEE Trans. Power Delivery,* vol. 13, no. 2, April 1998, pp. 596-604.
[6] A. Morched, B. Gustavsen, and M. Tartibi, "A universal model for accurate calculation of electromagnetic transients on overhead lines and underground cables", *IEEE Trans. Power Delivery,* vol. 14, no. 3, July 1999, pp.1032-1037.
[7] R. Koch and N. Gumede, "The impact of harmonic resonace conditions on the connection rules for larger industrial installations", *IPES 2005, Conference and Exposition in Africa* South Africa July 2005, pp. 320-325.
[8] N. Kaul and R. M. Mathur, "Solution to the problem of low order harmonic resonance from HVDC converters", *IEEE Trans. on Power Systems* vol. 5, no. 4, November 1990, pp. 1160-1167.
[9] J. J. Chavez and A. Ramirez, "Dynamic harmonic domain modeling of transients in three-Phase transmission lines", *IEEE Trans. on Power Delivery,* vol. 23, no. 4, October 2008 , pp. 2294-2301.
[10] E. Acha, and M. Madrigal, *Power Systems Harmonics-Computer Modeling and Analysis,* John Wiley & Sons, 2001.
[11] J. J. Rico, M. Madrigal, and E. Acha, "Dynamic harmonic evolution using the extenden harmonic domain", *IEEE Trans. on Power Delivery,* vol. 18, April 2003, pp. 587-594.
[12] B. Lu, X.Wu, H. Figueroa, and A.Monti, "A low cost real-time hardware in-the-loop testing approach of power electronics control", *IEEE Trans. on Industrial Electrocnics,* vol. 54, no. 2, April 2007 , pp.1235-1246.
[13] G. G. Parma and V. Dinavahi, "Real-time digital hardware simulation of power electronics and drives", *IEEE Trans. on Power Delivery,* vol. 22, no. 2, April 2007 , pp.1235-1246.
[14] RT-LAB 8.0 user manual Opal-RT Technologies, Inc., Montreal, QC, Canada, 2006.
[15] L.-F. Pak, M. O. Faruque, X. Nie, and V. Dinavahi, "A versatile cluster-based real-time digital simulator for power engineering research", *IEEE Trans. on Power Systems,* vol. 21, no. 2, May 2006 , pp. 1-11.
[16] V. Jalili-Marandi, Lok-Fu Pak, and V. Dinavahi, "Real-Time simulation of grid-connected wind farms using physical aggregation", *IEEE Trans. on Industrial Electronics,* vol. 57, no. 9, September 2010 , pp. 3010-3021.

Biographies

Jose de Jesus Chavez received his M.Sc. and Ph.D. from the Center for Research and Advanced Studies of Mexico (CINVESTAV) Campus Guadalajara, in 2006 and 2009 respectively. He is currently with Technological Institute of Morelia, Mexico. His interests are electromagnetic transient analysis in power systems, Harmonic analysis, and power electronic devices.

Manuel Madrigal received his Ph.D. degree from the university of Glasgow, Scotland in 2001. He is currently with the Instituto Tecnologico de Morelia, since 1996. His interests are power systems harmonics, Power quality, and Renewable energy.

Venkata Dinavahi received the Ph.D. degree in electrical and computer engineering from the University of Toronto in 2000. Currently, he is a Professor at the University of Alberta. His research interests include real-time simulation of power systems and power electronic systems, large-scale system simulation, and parallel and distributed computing.